A new interpretation of soft-sediment deformation features (SSDs) in the Parktown Formation (lower West Rand Group); the physical processes of deformation during deposition

K.A.A. Hein and L. Goslin
School of Geosciences, University of the Witwatersrand, Private Bag 3, 2050 Wits, South Africa
e-mail: kimhein61@gmail.com; 0000-0003-0264-0717; lechellegoslin@gmail.com; 0000-0002-4554-869X

Abstract

In the Parktown Formation of the lower West Rand Group (Witwatersrand Supergroup), remarkably well-preserved soft-sedimentary deformation features (SSDs) occur in a number of locations in three stratigraphic horizons across the Vredefort Mountainland and in key sites in Johannesburg. The SSDs were the inevitable products of static liquefaction during early deposition in the Witwatersrand Basin. The trigger to static liquefaction is interpreted to be autogenic and related to cyclic fluctuations in pore fluid pressure(s) during capped dewatering. Allogenic triggers are not indicated. We suggest that static liquefaction was an integral physical process to sediment deposition on the Parktown Formation offshore platform, but a process not previously recognised as important to the modification of the West Rand Group stratigraphy across the Witwatersrand Basin.

Introduction

The identification and classification of soft-sedimentary deformation features (SSDs) and their trigger mechanisms is presented by Allen (1982), Jones and Preston (1987), Maltman (1994), Maltman et al. (2000), Ettensohn et al. (2002) and others, but remains controversial. The terminology, nomenclature and interpretation of SSDs remains the subject of active research proving a challenge (Montenat et al., 2007; Owen et al., 2011), but has been extensively reviewed, critiqued and revised by Moretti and Van Loon (2014) and Shanmugam (2016; 2017). Certain key classification schemes have remained useful in aiding in the interpretation of SSDs and their meaning(s). These include classification systems of Potter and Pettijohn (1963), Allen (1982), Owen (1987) and Shanmugam (2017).

Importantly, the geological context and tectonic history of the SSDs plays a significant role in constraining possible trigger mechanics for a given set of field observations because SSDs are the direct products of sediment liquidisation and not (*per sē*) the triggers to liquidisation. However, the frequency, extent and type of SSDs implicate or discount certain environmental settings where the strato-tectonic relationships are well known, as is the case for lower West Rand Group (Vos, 1975; Camden-Smith, 1980; Watchorn, 1980; Stanistreet and McCarthy, 1991 and others).

By generally accepted definition, SSDs are those features that form in time with the earliest stages of sediment consolidation, non-tectonically, frequently close to surface, and/or shortly after sediment burial (Lowe, 1975; Allen, 1982; Owen et al., 2011 and others), and/or at a time when the sediment strength is weakest and pore fluid is expelled rapidly (Allen, 1982). As stated by Shanmugam (2017), the most accurate account of SSDs is given by Allen (1982) who stated that 'soft-sediment deformations arise shortly after (sometimes during) deposition, and reflect[ed] the deformable nature of freshly accumulated sediment, once a liquid-like state has been created through either liquefaction or fluidisation'. His characterisation of liquidisation as actioned by liquefaction (static, dynamic and cyclic) and fluidisation is adopted herein as being mechanisms by which SSDs are likely to have formed during early deposition of the lower Parktown Formation. The products of liquidisation in the lower Parktown Formation were liquified sediments and their SSD textures are (*sensu stricto*) pre-diagenetic (*c.f.*, Jackson, 1997).

Liquidisation is the loss of material shear strength (*sensu lato*) and a material change-of-state from solid to liquid, such that the material begins to behave as a viscous liquid (Allen, 1982; Rankka et al., 2004; Hansen et al., 2007; Boggs, 2011; Wang and Manga, 2021). A significant number of triggers are cited to induce liquidisation in geological settings including tectonic, glaciogenic, mass movement, sediment loading, sediment leaching, sediment mobilisation in deeply buried sediments, meteorite impact, and/or gravity collapse (Owen et al., 2011) with 21 possible trigger mechanisms reported by Shanmugam (2017).

Fluidisation occurs when externally supplied fluid is forced upward through the grain mass until fluid drag counteracts grain weight. This reduces the material strength resulting in failure (Allen, 1982). Fluidisation is associated with change in volume. This process commonly, but not exclusively produces clastic dykes and pillar structures (Owen and Moretti, 2011). Trigger mechanisms to fluidisation in geological settings may include floods, tidal surges, or expulsion of sub-surface reservoirs of gas and/or water.

In contrast, liquefaction as static, dynamic or cyclic mechanisms can be defined as the temporary or complete loss of strength as a result of the loss of grain-on-grain contact, effectively transferring the grain support to the pore fluid. The rising pore pressure reaches the magnitude of the overburden (confining) pressure, and the sediments lose strength to become fluid-like and liquefy. There is no dynamic inflow of fluid into the system or change of volume as occurs with fluidisation; any fluid flow inward is purely passive (Allen, 1982).

The mechanism of static liquefaction occurs when the rising pore pressure reaches the magnitude of the overburden (confining) pressure in a stationary mass of sediment, and failure ensues. The static load is the trigger mechanism. Quick clay failure is a special type of static liquefaction in which leaching of the clay by meteoric water changes the ion concentration of pore waters (Rankka et al., 2004) and ultimately its shear strength. The mechanism of dynamic liquefaction is short-lived and typically restricted to a single time event involving overloading or shock, such as explosions, the fall of massive bodies, tsunami or tidal bore waves. In contrast, the mechanism of cyclic liquefaction associates with repeated reversal of load over time, as is common to wave action, tremors-earthquakes (Wang and Manga, 2021), and failure of tailings and water storage dams when dams are cyclically recharged.

Alternatively, triggers to liquefaction can be subdivided into allogenic and autogenic as discussed by Owen and Moretti (2011) and Owen et al. (2011). Allogenic triggers are external to the depositional environment and far-field, while autogenic triggers are part of the depositional environment. Allogenic triggers in geological environments are invariably linked to ground-motion regardless of whether the ground-motion was consequent of volcanism and/or sub-volcanism, earthquake seismicity related to plate tectonics, meteoric impact, or mechanical vibration induced by during construction or mining. The magnitude and intensity of ground-motion is measured seismically (*c.f.,* Shanmugam, 2016).

This research reports on the types, distribution and occurrences of SSDs in outcrops of the Parktown Formation at selected sites in the Vredefort Mountainland and City of Johannesburg (Figure 1). The SSDs are reasonably interpreted as the products of liquidisation by either fluidisation or static-dynamic-cyclic liquefaction. Possible trigger mechanisms to liquidisation are evaluated against the geological context and environmental setting presented by Stanistreet and McCarthy (1991), Frimmel and Minter (2002), Dankert and Hein, (2010), Manzi et al. (2013), Molezzi (2017), Molezzi et al. (2019). The SSDs and their host rock units are couched within the broad context for deposition in the lower West Rand Group in the Witwatersrand Basin.

The primary goal of mapping in the key localities was:

- to establish the nature, character and extent of SSDs in the Parktown Formation,
- to contextualise the SSDs within the overall stratigraphic framework of the Parktown Formation, particularly with respect to the 'Contorted Bed' of Fripp and Gay (1972) and Mayer and Albat (1990);
- to consider continuity along strike of the mappable units, and
- to evaluate the SSDs in light of controversies surrounding of the triggers to SSDs and their relationship (or not) to tectonism.

In this paper, the term 'psuedonodules' of Macar (1948) is used herein in revision of 'ball-and-pillow' of Potter and Pettijohn (1963), as recommended by Owen (1978) to refer to subrounded masses of clastic sediment set in a similar to finer grained matrix. Pseudonodules are divided into:

- attached psuedonodules that reflect the progression from load casts to strings-of-nodules along a bedding plane, or
- detached psuedonodules that are isolated for remnant bedding.

Detached psuedonodules may occur as drop-down or sag-down lithons into underlying fine sediment layers that liquify during shear-thinning.

Geological setting

The West Rand Group of the Mesoarchean Witwatersrand Supergroup (South Africa) (Figure 1) is interpreted to be an epicontinental cover sequence for which depositional models generally describe a stable tidal to marine environment (Vos, 1975; Camden-Smith, 1980; Watchorn, 1980; Stanistreet and McCarthy, 1991 and others). Initiation of the Witwatersrand Basin at *ca.* 2.98 Ga in the lower West Rand Group and concomitant deposition of argillaceous and arenaceous sediments in the Parktown Formation is interpreted to indicate that deposition took place in a transgressive, tide-dominated environment (Stanistreet et al., 1986).

The protolith of the West Rand Group (minimum age of 2 914 ± 8 Ma, Armstrong et al. 1991) is composed of Fe-rich greywacke units, with magnetite-bearing iron formations; these are interbedded with arenite and diamictite units (McCarthy, 2006). Deposition in the West Rand basin was terminated during partial basin inversion in the Asazi Event (Manzi et al., 2013),

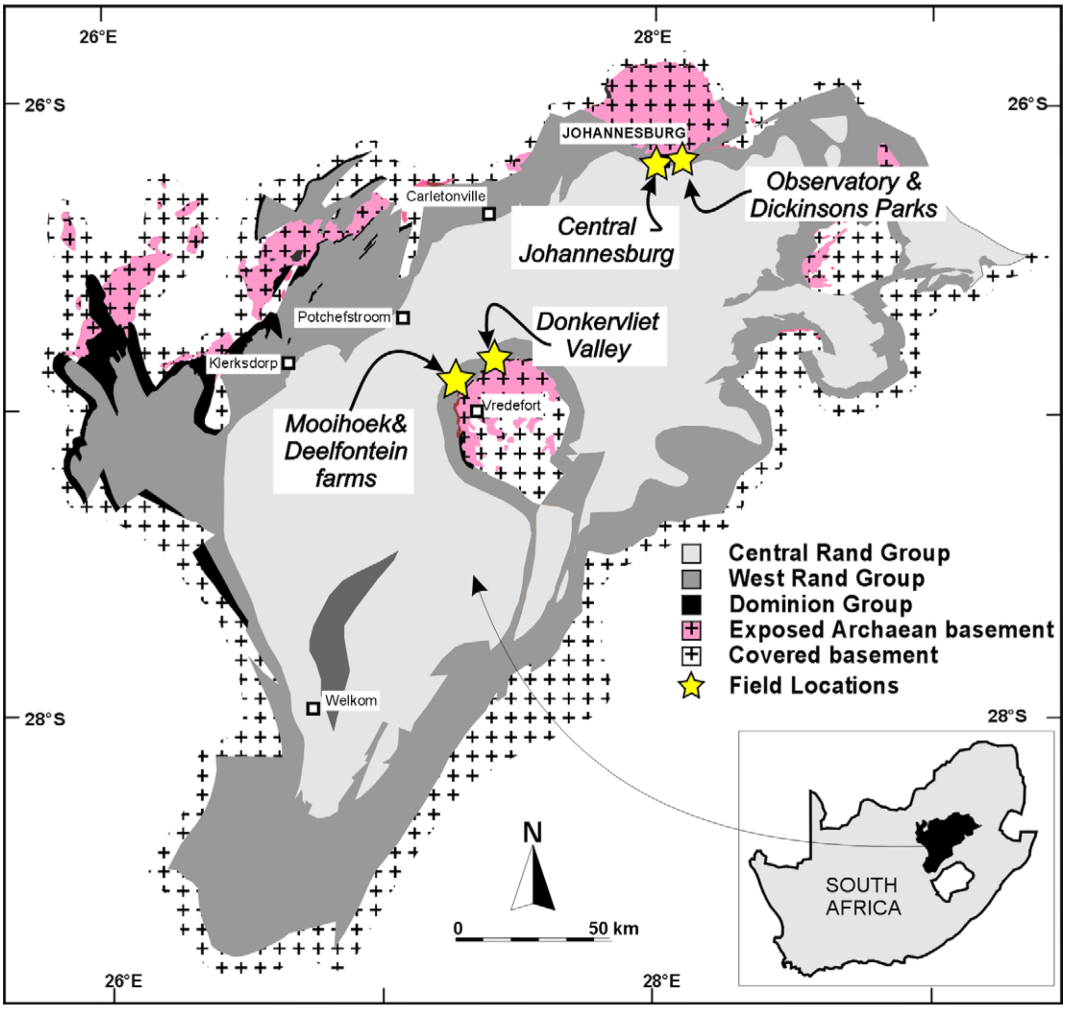

Figure 1. *Schematic geological map of the Witwatersrand Basin (South Africa) with Ventersdorp Supergroup, Transvaal Basin sequences and Karoo Supergroup cover removed (modified after Pretorius et al., 1986). The distribution of (surface and subsurface) Archaean basement and location of goldfields, after Pretorius et al. (1986) is presented. Field study sites in the Vredefort Mountainland and City of Johannesburg marked as stars.*

and prior to unconformable to conformable deposition of the Central Rand Group (*ca.* 2 902 to 2 849 Ma; Kositcin and Krapež, 2004; U-Pb detrital zircon SHRIMP), which is composed of quartzites interbedded with metapelites and thin (economic) gold-bearing meta-conglomerate reefs.

The Parktown Formation in the lower West Rand Group is interpreted to represent deepening and seaward extension of the basin into a passive margin by progradation of distal shelf deposits (Watchorn, 1980; Camden-Smith, 1980; McCarthy, 2006; Nwaila et al., 2017; Frimmel, 2019). Rare trough-cross beds and bidirectional flow indicators display northwest-southeast and east-west paleocurrent directions, which are consistent with tide-dominated environments (Watchorn, 1980).

Subsequent and during deposition, the sedimentary sequences of the Witwatersrand Supergroup were subjected to several phases of metamorphism and attained greenschist to mid-amphibolite facies during:

- emplacement of dykes, sills and lavas of the bimodal tholeiitic basalt-dacite suite of the Ventersdorp Supergroup (*ca.* 2.72 to 2.63 Ga) (Beaton et al., 2022);
- strato-tectonic inversion during formation of the Vredefort meteorite impact crater at *ca.* 2020 million years ago (Reimold and Gibson, 2006), and
- distal emplacement of the Bushveld Complex mafic layered intrusion (*ca.* 2.06 Ga) (Beaton et al., 2022).

Remarkably, primary sedimentary and SSDs were preserved as compositional layering, but with development of cordierite, andalusite, biotite, staurolite, magnetite and garnet metamorphic mineral assemblages (Stevens et al., 1997; Beaton et al., 2022).

In 2011-2012, numerous SSDs were identified during student field studies in the Vredefort Mountainland in the lower Parktown Formation of the West Rand Group (Figures 1 to 4). At that time, they were classified as slump-induced pelites or diamictites (and perhaps temporarily forgotten) with questions as to whether certain outcrops marked the position of the so-called Contorted Bed of SACS (2006). Subsequent to a new round of field studies, a significant number of SSDs were identified in outcrops at locations across several sites in the Vredefort Mountainland and the City of Johannesburg. These sites became the focus of detailed field study and map work to further evaluate the depositional environment of the Parktown Formation and compare that data with depositional models for the lower West Rand Group.

The protolith composition and stratigraphic divisions of the Parktown Formation have been reported by Fripp and Gay (1972), Camden-Smith (1980), Smith et al. (2013), SACS (2006) and others, with studies of iron formations internal to the Parktown Formation by Smith et al. (2008; 2013) and Viehmann et al. (2015). The stratigraphy of the Parktown Formation in the selected sites of study is summarised in Figure 2.

Although the Parktown Formation shows some variation across the Witwatersrand basin, it is generally accepted that the formation marks a shift from a dominantly tidal marine environment in the basal Orange Grove Quartzite to offshore marine in the Parktown Formation (Camden-Smith, 1980). Deposition of the Parktown Formation is thereby dominated by intercalated carbonaceous siltstone-shale-banded iron formation (BIF) ± greywacke ± chert beds, and an increase in iron content as marked by the Water Tower Shale Member (SACS, 2006; Smith et al., 2013; Nwalia et al., 2017) and the Contorted Bed (SACS, 2006; Hospital Hill slates of Hatch and Corstorphine, 1905) or Contorted Bed iron formation of Smith et al. (2013). The Water Tower Shale Member, although mostly iron-rich shale, can contain iron formations in some locations (Smith et al., 2008; 2013; Viehmann et al., 2015).

Beds lower in the Parktown Formation are ferruginous and carbonaceous. Interbeds of arenite and lithic-arenite such as the Bulskop or Brixton Quartzite break the sequence (*c.f.*, the Rippled-marked Quartzite of Hatch and Corstorphine, 1905). Smith et al. (2013) interpreted these breaks as cycles associated with marine regressions.

An approximately 120 m-thick Fe-rich shale-siltstone horizon overlays the Bulskop quartzite (Camden-Smith, 1980). The Fe-rich shale-siltstone horizon is divided into sub-units separated by a thin discontinuous sub-lithic arkose (Hatch and Corstorphine, 1904), namely:

- a lower package of laminated Fe-rich shale-siltstone-greywacke beds, and

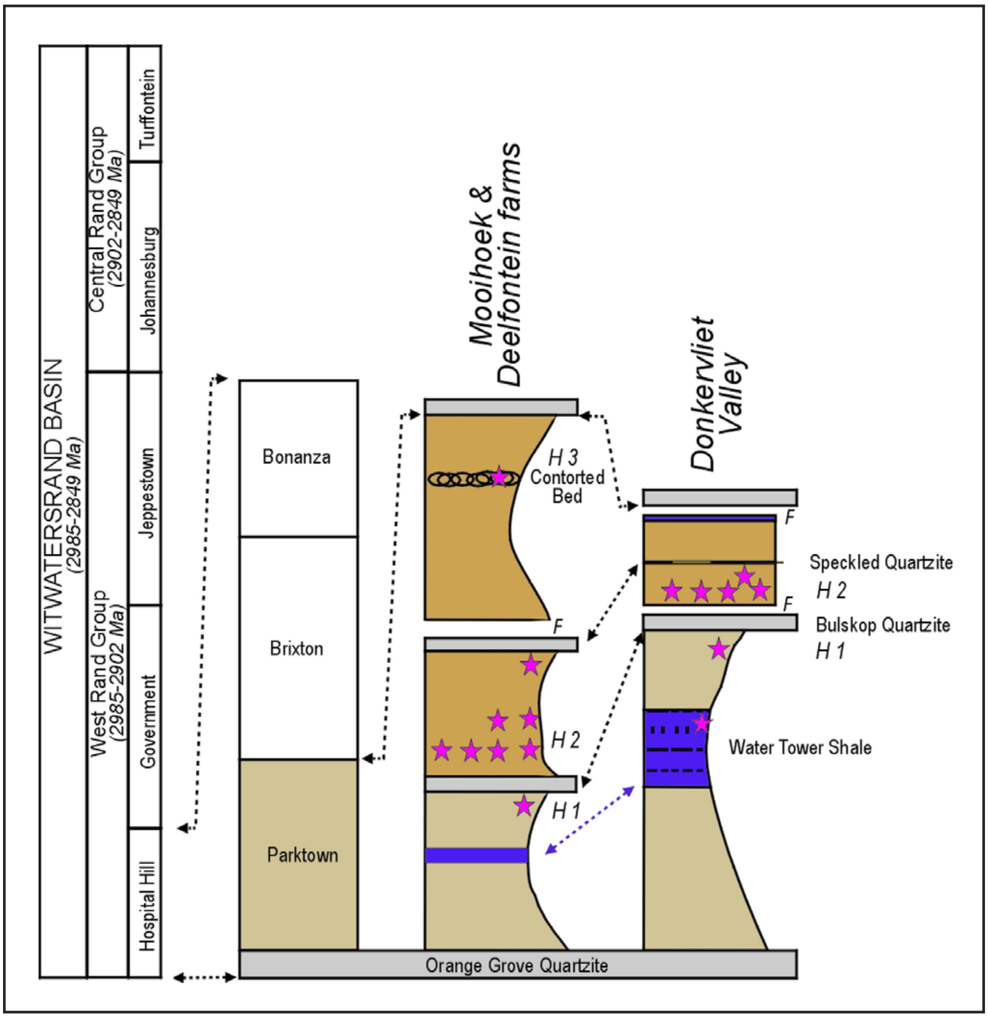

Figure 2. *Schematic stratigraphic profile of the Parktown Formation in the lower West Rand Group. The Hospital Hill Subgroup marks the base of the West Rand Group; it is divided into the Orange Grove Quartzite (2 849 ± 18 Ma; Kositcin and Krapež, 2004; U-Pb detrital zircon SHRIMP), Parktown, Brixton and Bonanza (2 990 ± 8 Ma) formations. Soft-sediment deformation features (SSDS) (magenta stars) occur throughout the Parktown Formation but dominate three stratigraphic horizons (H1 to H3). The Contorted Bed in Donkervliet Valley is absent due to faulting (F).*

- an upper package of intercalated Fe-rich shale, iron formation, rippled-marked siltstone and sandstone.

In the study areas, the horizon above the Bulskop Quartzite preserves numerous soft-sedimentary features and textures in the lower Fe-rich shale-siltstone-greywacke beds that are consistent with liquefaction of the protolith during deposition.

In contrast, the upper package preserves rare SSD iron balls and iron casts in the Vredefort Mountainland. However, Hatch and Corstorphine (1905), Camden-Smith (1980), SACS (2006), Smith et al. (2013) and others, place a regional stratigraphic marker termed the Contorted Bed in the upper series. The nature and character of the Contorted Bed are subjects of discussion and contention in historic literature.

The Parktown Formation is overlain by the massive, coarse grained litharenites of the Brixton quartzite in the Brixton Formation (*c.f.*, *RHq3* quartzite of SACS, 2006). The quartzite is herringbone and trough cross-bedded with fuchsite along bedding planes (Mashabela, 2016).

Methodology

Field studies and mapping took place in the Vredefort Mountainland on the Donkervliet Eko and Avontuursentrum (Figure 3), Mooihoek and Deelfontein farms (Figure 4) because they offered excellent outcrop exposure, permission to access, and continuity of mappable units. Limited mapwork at selected sites in the City of Johannesburg included;

- outcrops of the Parktown Formation at the Observatory and Dickinson parks, which are located 5 km northeast of central Johannesburg, and
- road cuts east of the University of Witwatersrand in central Johannesburg on Jan Smuts Avenue and Melle Street, which where previously mapped by Fripp and Gay (1972) as a key location for the Contorted Bed (Figure 2).

Nine traverses were conducted across the Parktown Formation to constrain stratigraphic relationships. They were terminated at crosscutting shear-faults in order to compartmentalise the stratigraphic sections within clearly defined and mappable blocks. Depositional models were developed on the basis of sedimentary textures within specific lithological units. Samples of pertinent outcrops were collected to characterise the SSDs and provenance of the host protolith.

Study sites

The location of the study sites is presented in Figures 1 to 4 with detailed maps and generalised stratigraphy for the Donkervliet Valley and the Mooihoek and Deelfontein farms in the Vredefort Mountainland in Figures 3 to 4. Site locations at Observatory-Dickinsons Geo-parks, Jan Smuts Avenue and Melle Street in Johannesburg were studied as duplicate of the Water Tower Shale in the lower Parktown Formation, and to study the Contorted Bed, which was not outcropping at Vredefort.

The Donkervliet Valley site is located on the north-northwest margin of the Vredefort Dome and is currently part of the Vredefort Geo-reserve. It is approximately 3.5 km long on an east-southeast axis, and 1.3 km wide (Figure 3). The geology in the Donkervliet Valley is generally made up of metamorphosed deltaic sedimentary rocks that are crosscut by narrow dolerite dykes. Metamorphism attains mid-amphibolite facies with cordierite, biotite, andalusite and rare garnet indicator metamorphic minerals (0.5 to 3 cm in size), but primary textures and SSDs are well-preserved as compositional layering throughout the valley and in the contact aureole of dolerite dykes.

The protolith sediments in Donkervliet Valley show interlayering between fine-grained marine pelites, turbidites, and medium-grained beach arenite to litharenite, but outcrops of intercalated greywackes occur across the valley. The rocks are generally overturned and steeply inclined (average bed strike and dip of 078°/66° south-southeast), which facilitated field mapping. Stratigraphic facing (up stratigraphy) is to the north-northwest across the Parktown Formation as established from bed gradation in turbidites and cross-bedding in arenites; prominent quartzite ridges of the Orange Grove Quartzite and Brixton Formation mark the south-southeast and north-northwest ridge boundaries, respectively (Figure 3).

The south-southeast flank of Donkervliet Valley is dominated by compositionally layered, dark brown to black Fe-rich pelites (1 000 m) including the Water Tower Shale Member (*c.f.*, SACS, 2006). The Water Tower Shale Member displays local scour and fill textures, minor crossbedding within arenite interbeds, turbiditic gradation, psuedonodules and floating lithons. Alternating iron and chert-rich layers as BIF exhibit small-scale folds as SSDs. Minor slump features in this unit display compaction and dewatering textures including minor load casts, microfaults and ptgmatically folded sand dykes. These are gradational into the overlying 20 to 30 m thick Bulskop Quartzite.

The Bulskop Quartzite, which is regionally known as the Rippled-marked Quartzite (SACS, 2006) displays minor crossbedding and ripple marks. The intense orange colour of the weathered surface and negative cube facets (after pyrite) are notable characteristics of the Bulskop Quartzite in Donkervliet Valley. The upper contact of the Bulskop Quartzite is marked by a minor late shear-fault whose displacement could not be established during field mapping.

Fe-rich pelites and greywacke interbeds (120 m) unconformably overlie the Bulskop Quartzite in Donkervliet Valley, and these host numerous SSDs. The SSDs include dewatering channels (Figures 5a, d and e), chaotic bedding (Figures 5b to e), pseudonodules (Figure 4, 5b, 6c to f), small and large-scale sedimentary dykes (Figures 5b to c, 6b to d and 7a), floating lithons (Figures 5d to e and 7c), bed-scale syn-sedimentary faults (Figure 7d), rare load casts, and slump folded beds (Figures 8a to c). An increase in SSDs was observed in the greywacke up stratigraphy. The Fe-rich pelites and greywacke interbeds are overlain by a discontinuous (0.5 m) arkosic quartzite member that elsewhere is termed the Speckled Quartzite (*c.f.*, Hatch and Corstorphine, 1905; SACS, 2006). It is mostly absent in the Donkervliet Valley meaning the Fe-rich pelites and greywacke interbeds are possibly unconformably overlain by iron formations.

A bed parallel fault terminated the end of the traverses at the position of the upper iron formations. The fault is marked by quartz vein fragments, fault gouge, and distinct epidote-chlorite

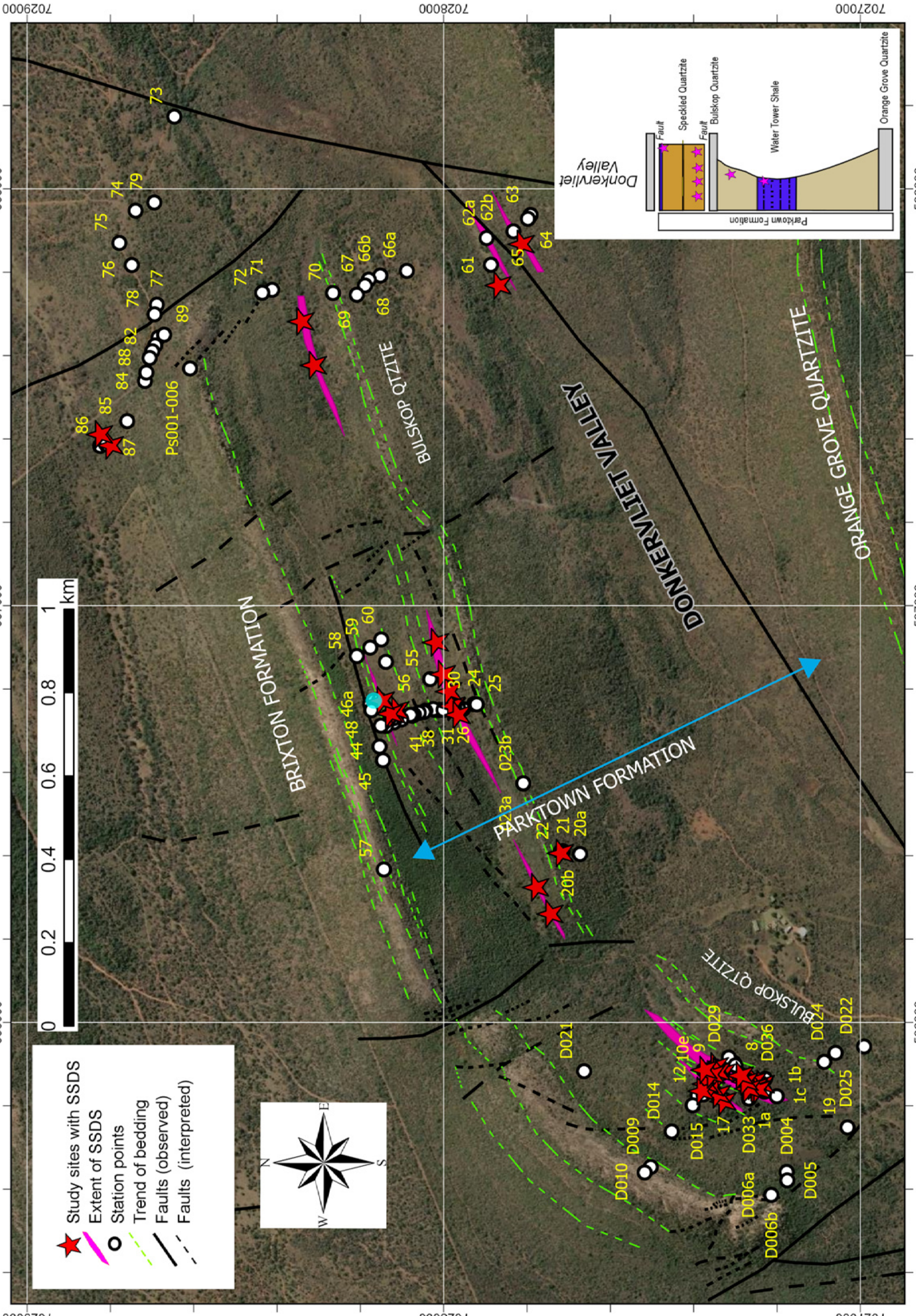

Figure 3. Google Earth image of field sites mapped at the Donkervliet Eko and Avontuursentrum in Donkervliet Valley in the Free State (South Africa), with generalised stratigraphic profile of the Parktown Formation in the valley. Field data layers were generated in UTM coordinates in ArcGisPro. Field data was collected along three traverse lines (western, central and eastern lines) across the valley, from the Orange Grove Quartzite in the south-southeast to the Brixton Formation in the north-northwest. Bedding trends east-northeast and dips steeply north-northwest or is steeply overturned. Stratigraphic facing (up stratigraphy) is to the north-northwest.

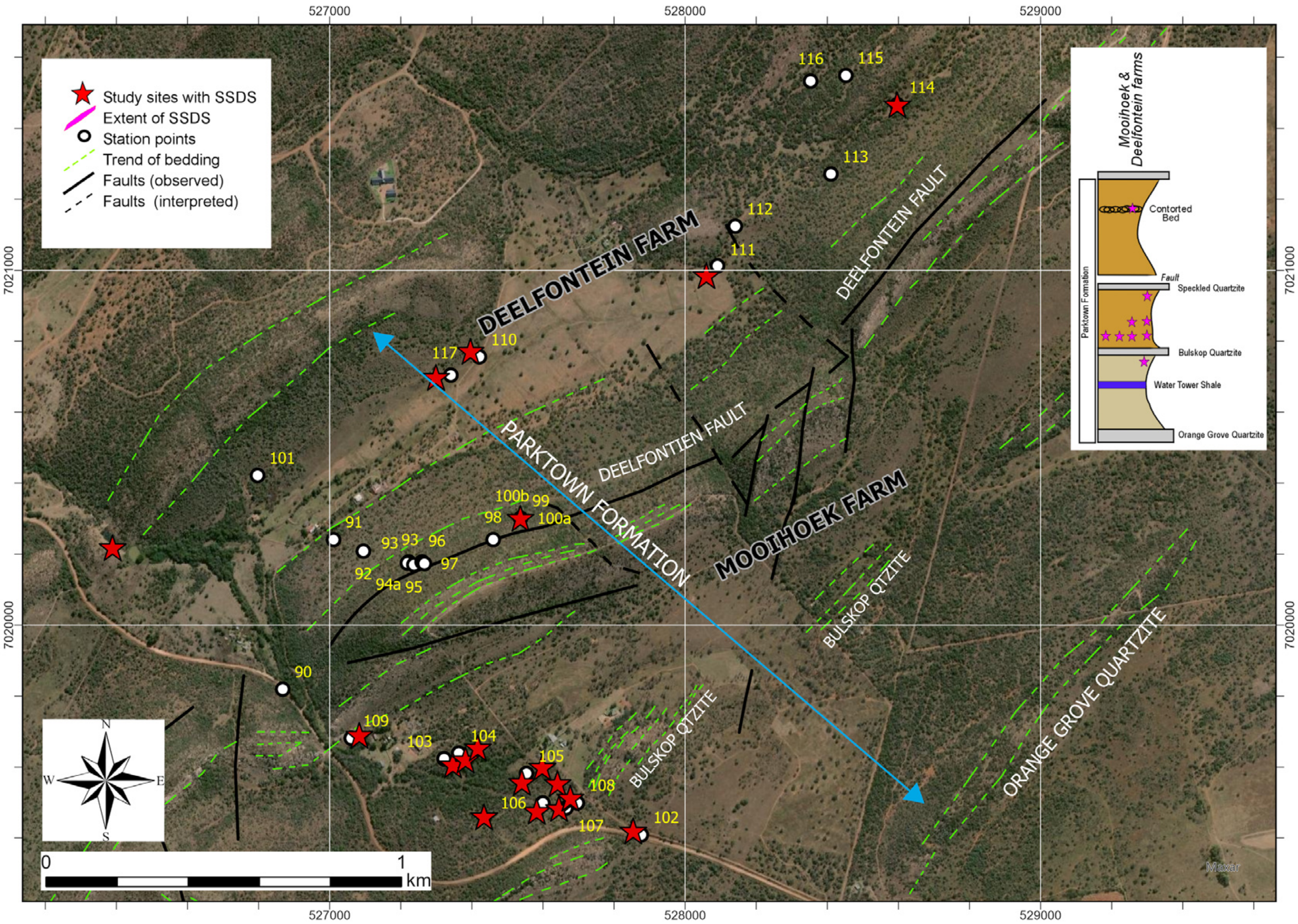

Figure 4. Google Earth image of field sites mapped at the Deelfontein and Mooihoek farms in the Free State (South Africa), with generalised stratigraphic column for the Parktown Formation on the farms. Field data layers were generated in UTM coordinates in ArcGisPro. Field data was collected along two traverse lines (western and central lines) across the valley, from the Orange Grove Quartzite in the southeast on the Mooihoek Farm to the Brixton Formation in the northwest on the Deelfontein Farm. Bedding trends northeast and dips steeply north-northwest or is steeply overturned. Stratigraphic facing (up stratigraphy) is to the north-northwest.

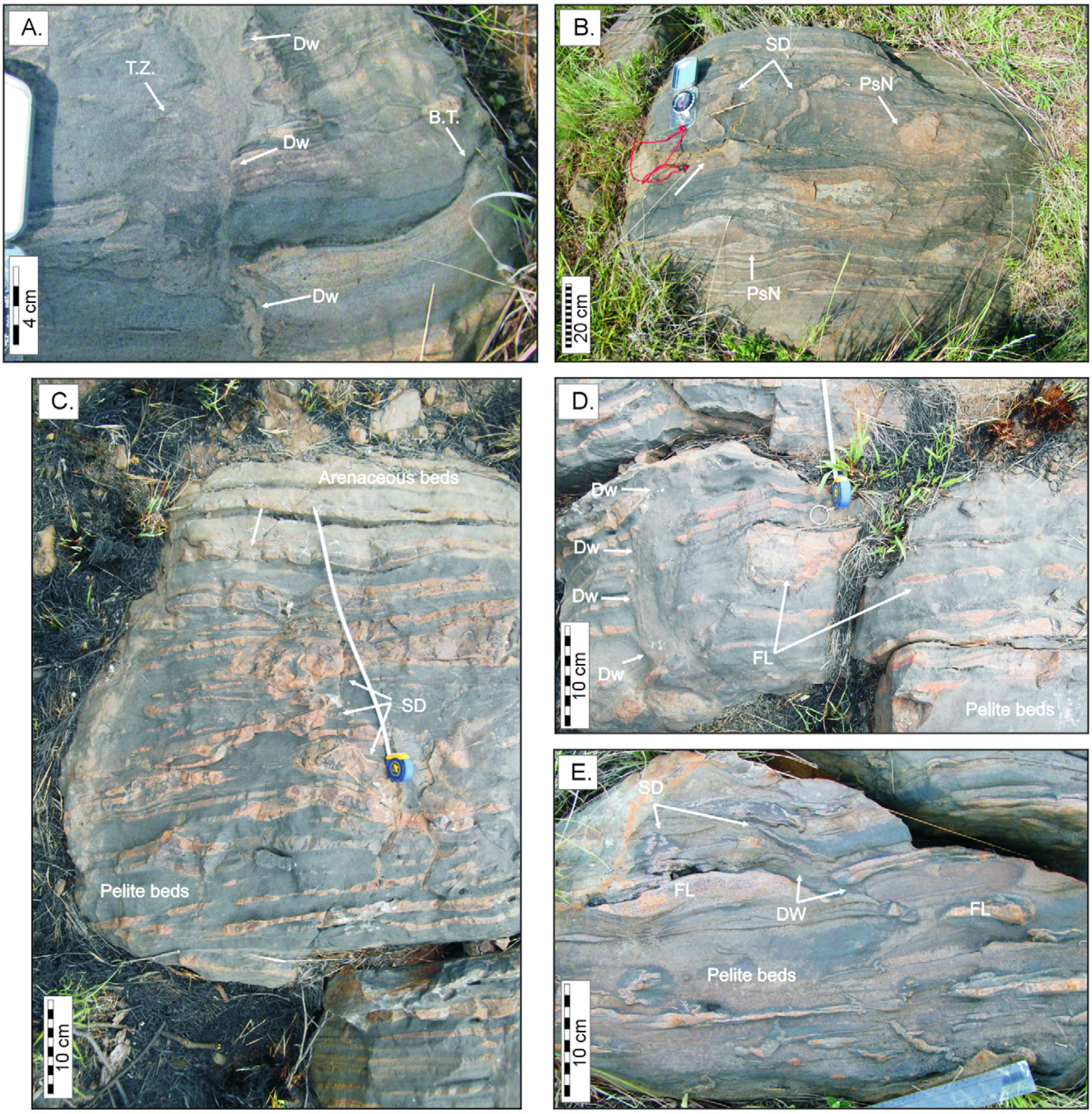

Figure 5. *(**A**) Dewatering channels (Dw) crosscut and disrupt heterolithic greywacke-pelite layers. Zones of turbulence (T.Z.) occur along the dewatering channels and create lobate bed parallel projections of the channels (UTM 35J, 535879 7027331). (**B**) Chaotic bedding results when unconsolidated sand injects through pelite layers to allow sand layers to dewater. Psuedonodules (PsN) bulge upward through the pelite layers, and sand dykes (SD) crosscut over tens of centimetres of stratigraphy (UTM 35J 535816 7027329). (**C**) Fine (orange) unconsolidated arenite layers are disrupted and remobilised to form complex syn-sedimentary sand dyke-sill-fold architectures and chaotic bedding (UTM 35J 535855, 7027242). (**D**) Dw disrupted bedding. In extreme liquidization of the sediments, arenite beds are dismembered to create floating lithons (FL). These form bed thinning and simple shear along bedding planes during compaction (UTM 35J, 536748 7028045). (**E**) Bed compaction and shear thinning associates with early formation of micro-faults that ultimately become Dw. The layers are dismembered and displaced accordingly, and then remobilised into SD.*

alteration along its trace. Above this fault, iron formations grade to siltstone, and into quartzite of the Brixton Formation.

In comparison, the Deelfontein and Mooihoek farms are situated on the northwest margin of the Vredefort Dome 12 km southwest of the Donkervliet Valley on the westward continuation of the Parktown Formation (Figures 3 and 4). The farms are separated by the Deelfontein Fault (3 m-wide) that was mapped during this study, and the Speckled Quartzite (SACS, 2006).

The Mooihoek Farm to the south of the Speckled Quartzite is crosscut by sheeted dolerite dykes and attains greenschist to amphibolite facies metamorphism in the contact aureole of the intrusions. The Orange Grove Quartzite marks a low ridge on the southwest farm boundary. A 600 m-wide scree-slope marks the position of Fe-rich pelites, thin (±5 to 10 m) iron formations and the Water Tower Shale Member, which grades into faulted segments of the Bulskop Quartzite (50 m) (Figures 2 and 3). SSDs identical to those found in Donkervliet Valley are prevalent over 100 to 120 m of stratigraphic interval in a 400 m-thick package of greywacke and Fe-rich siltstone between the Bulskop Quartzite and Speckled Quartzite. SSDs include relic

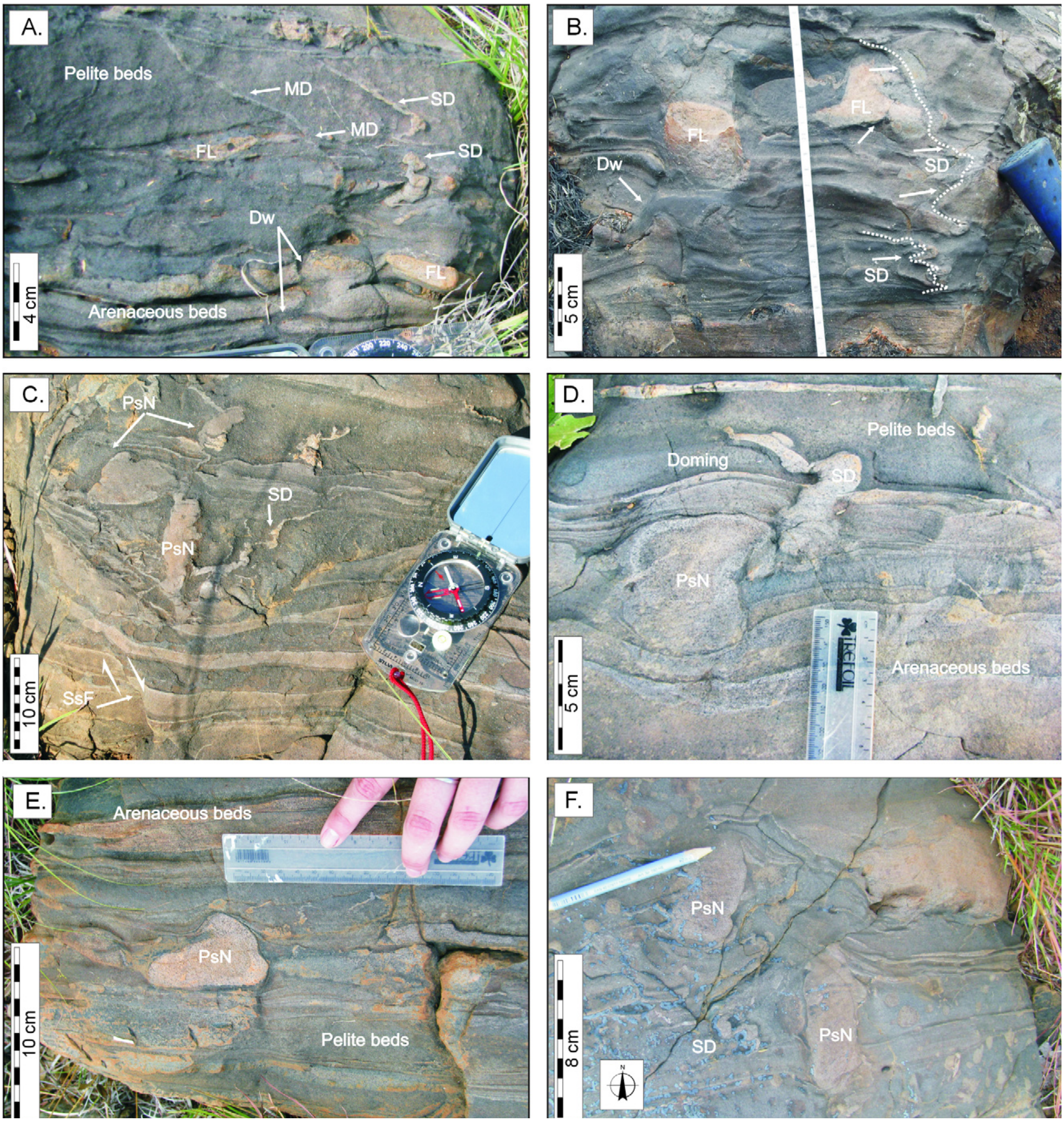

Figure 6. *Soft-sediment deformation features (SSDS) recognised in, (**A**) the complex arrangements of SSDS include dewatering channels (Dw) through arenaceous beds, floating lithons that are the result of bed dismemberment and sag-down, and generations of sand dykes and mud dykes. The sand dykes (SD) are ptgmatically folded from progressive compaction (UTM 35J 535874 7027286), (**B**) The complex relationship of dewatering and SD is such that the original bed orientation is totally lost. In this case, liquidisation is extreme and sand lithons sag-down into the slurry base (UTM 35J 536750 7028010), (**C**) and (**D**) SDs may also bulge and fatten as they inject upward into pelite to form pseudonodules (PsN), or begin as diapiric eruptions from underlying water-saturated arenaceous beds. Diapiric eruptions typically cause overlying bed to dome upward. Syn-sedimentary micro-faults (SsF) facilitate dewatering of lower bed layers (UTM 35J 535880 7027342; 536824 7028033), (**E**) and (**F**) Detached PsN are the extreme case of liquidisation in which the original sediment layer in transposed into dyke or diapiric PsN (UTM 35J 536730 7028120; 536919 7028150).*

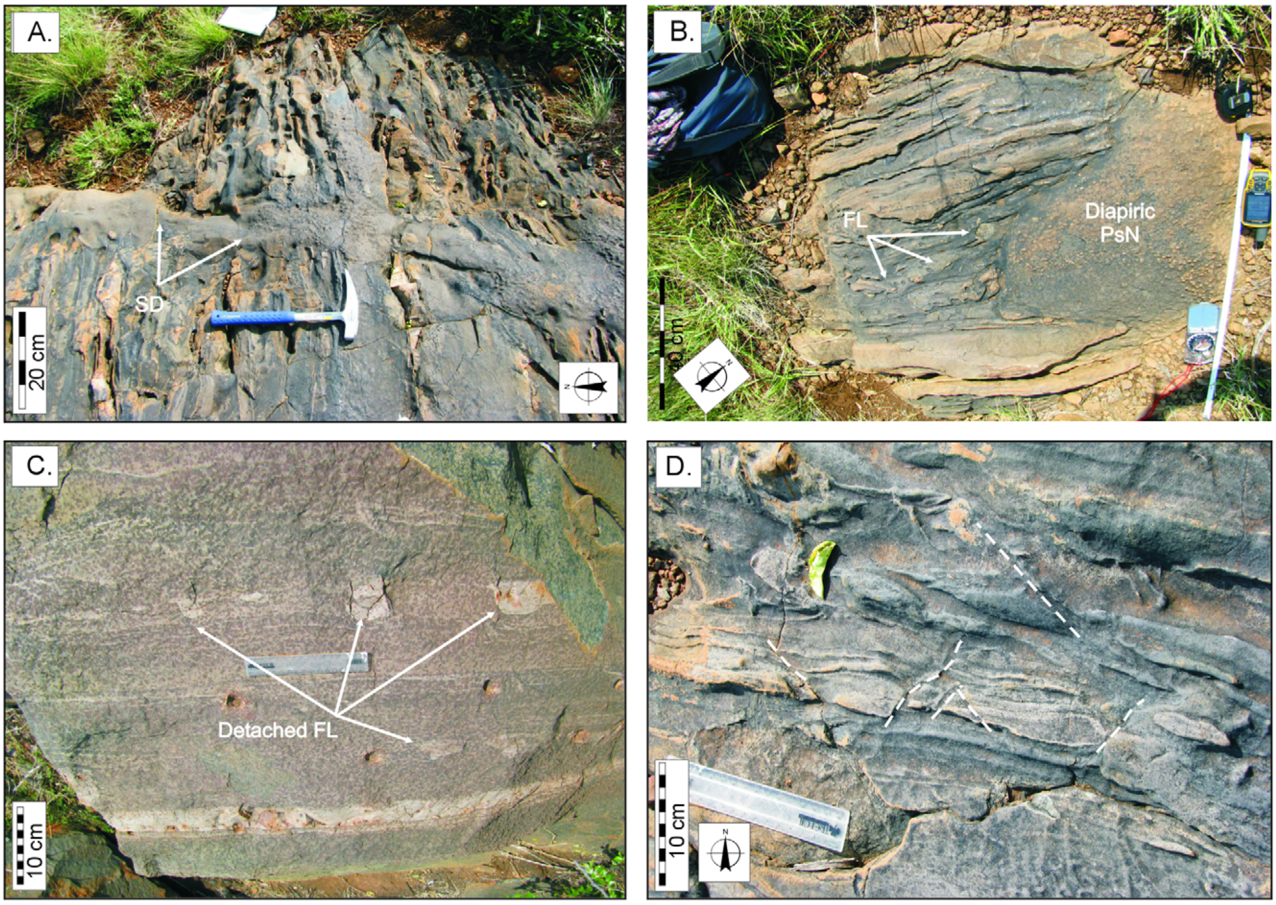

Figure 7. *(**A**) Sedimentary dykes in the field areas may inject through multiple layers for several metres and inject to form short sills or (**B**) diapir bulges along bedding planes (UTM 35J 536879 7028209; 535841 7027360). (**C**) Detached floating lithons (FL) form as a result of shear thinning and dismemberment of beds during liquidisation (UTM 35J 536772 7028168). (**D**) Micro-faulting or necking of layers to is a form sedimentary boudinage that result from gravity-driven compaction. It can be found in all study sites (UTM 35J 536879 7028209).*

pseudonodules, floating lithons, ptgmatically folded sedimentary dykes, chaotic bedding, detached and fragmented bedding, pseudonodules and attenuated beds.

The Deelfontein Farm on the north side of the Deelfontein Fault and Speckled Quartzite is characterised by greenschist facies metamorphic assemblages in an 840 m-thick package of BIF and Fe-rich siltstone-shale. Outcrops are few and SSDs infrequent. Thin arenite beds intercalate with red to dark-brown shale (metapelite) and magnetic iron formations. The pelites display relic sand layers or isolated sand lithons. The lithons are laminated or cross-bedded with heavy minerals along relic bedding planes. Minor fold convolutions and chaotic bedding in Fe-rich shale are interpreted to mark the position of the Contorted Bed of SACS (2006).

In regard to field sites in Johannesburg, the Observatory-Dickinsons parks sites are situated 5 km east of Johannesburg Central on outcrops of the Water Tower Shale. These sites were included in comparison of the Vredefort Mountainland sites. SSDs in the shale included minor sand floaters and convoluted bedding. The shales are gradational into greywacke, polymictic lithic greywacke and oligomictic diamictite.

The north-south road-cut exposures along Jan Smuts Avenue (200 m-long) and Melle Street (50 m-long) in central Johannesburg were chosen to examine the Contorted Bed (Figures 8a to c), as described by Hatch and Corstorphine (1905) and mapped by Mellor (1911), and because the Contorted Bed was not exposed at other study sites. Hatch and Corstorphine (1905), Camden-Smith (1980), SACS (2006), Smith et al. (2013) and others, mapped the Contorted Bed as a regional marker. Arguments for a tectonic rather than sedimentary origin of the contortions in the Contorted Bed are presented by Fripp and Gay (1972 after Struben, 1885, Penning, 1891 and Draper, 1896) and Mayer and Albat (1990), with conclusions that the contortions of this marker is tectonically induced. The sedimentological origins for the formation of the Contorted Bed are presented by Truswell (1970) who argued that disharmonic folds in the beds represented slump-induced folding and were thus syn-sedimentary.

On their northern extent, road-cuts along Jan Smuts Avenue (200 m-long) and Melle Street (50 m-long) expose a series of southerly vergent tectonic folds above a basal (small-scale) decollement that crosscut carbonaceous siltstone-shale-BIF beds

(Fe-rich pelites), as described by Fripp and Gay (1972). Penetrative steeply north-dipping axial planar cleavages and small-scale fold-thrusts are present above a basal decollement, with reverse displacement on thrust planes (north block up). However, it is clear from crosscutting relationships that the carbonaceous siltstone-shale-BIF beds were slump-folded prior to tectonic folding, as evidenced along the central and southern extent of the roadcuts by the refolding of the slump folds and other SSDs. SSDs included small-scale load casts, thinned beds, composite slump folds and rolls (metre-scale) (Figures 8a to c), local chaotic bedding near slump folds, rare micro-dewatering channels and turbidites. The SSDs are comparable to those

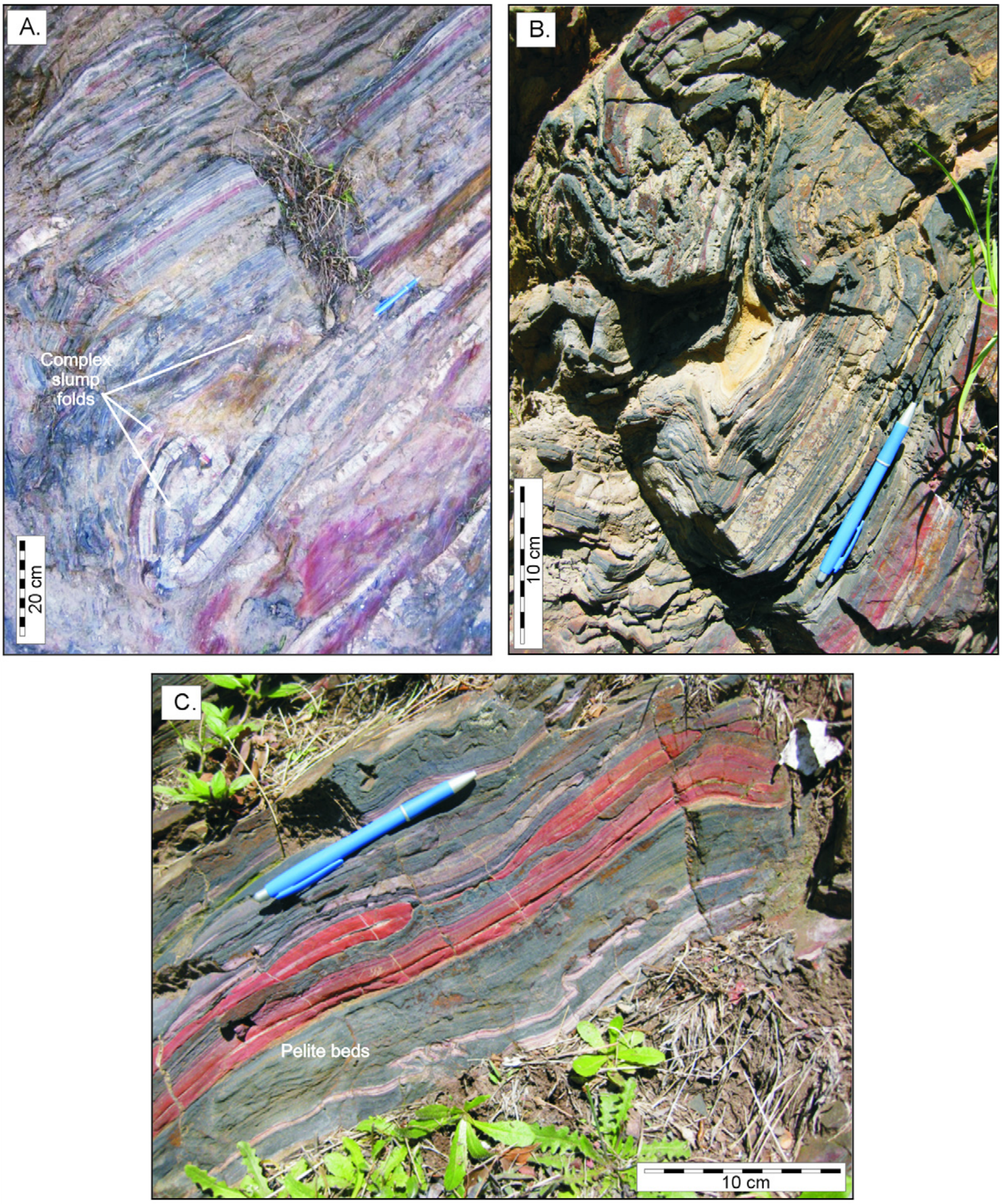

Figure 8. *Photographs of slump folds of the Contorted Bed of Hatch and Corstorphine (1904), Mellor (1911) and Fripp and Gay, (1972) and SACS (2006) as seen in north-south road cut along Jan Smuts Avenue adjacent to the University of the Witwatersrand in Johannesburg. The view is to the east. Although tectonically folded on the northside of the road cut, slump folds of various scales, and minor soft-sedimentary features may be found in the outcrops. Photographs are courtesy of C. Bentley, with written permission.*

found at Donkervliet Valley and Mooihoek Farm, but should not be confused with crosscutting younger tectonic features found in those locations, such as faults and fold-thrusts.

Soft-sediment deformation (SSD) textures

The SSDs in the study areas are generally restricted (but not exclusively) to three stratigraphic horizons within the Parktown Formation, namely:

- Horizon 1 – carbonaceous Fe-rich chert-rich layers and the Water Tower Shale below the Bulskop Quartzite (Ripple-marked Quartzite),
- Horizon 2 – Fe-rich greywacke-siltstone-shale layers between the Bulskop and Speckled quartzites, and,
- Horizon 3 – carbonaceous siltstone-shale and BIF between the Speckled Quartzite and first quartzite of the Brixton Formation (i.e., the Contorted Bed iron formation).

In these horizons, pinch-and-swell textures and load casts are found at the base of partially consolidated or well-packed low porosity beds (e.g., siltstone or sandstone beds). Vertical to sub-vertical fracture-faults formed at pinch points leading to development of centimetre to decimetre-scale lithons and boudins, and in extreme cases, formed isolated floating lithons and pseudonodules. Micro-faulting, shear thinning and fragmentation was part of the dynamic syn-sedimentary process at all study sites.

At the same time, unconsolidated water-saturated beds appear to have liquified and flowed leaving lithons to float or sag-down into liquified slurry. The field outcrops show that integrity of the bedding was lost during liquidisation with evidence of turbulent flow. Dewatering marks and channels, small-scale sand dykes and chaotic beds occur at all study sites and were formed as bed layers reorganised. Crosscutting dewatering channels and sand dykes point to multiple stages of liquidisation within a single horizon, particularly Horizon 2. In Donkervliet Valley, pseudonodules, metre-wide sedimentary dykes and sills, and metre-scale lapolithic-type bulges occur as end-member SSDs in Horizon 2; the metre-wide sedimentary dykes and sills indicate strong liquidisation of the horizon.

The SSDs in the outcrops at Donkervliet Eko Avontuursentrum, Deelfontein and Mooihoek farms are dominated by two textural types, namely:

- dewatering features and plastic injections related to bed loading and concomitant liquidisation of the sedimentary pile, and;
- convolutions and slump folds related to simple shear along beds during liquidisation.

Dewatering features are millimetric in width up to metre wide in the study areas.

Chaotic, fragmented and floating beds

Chaotic bedding is the rearrangement of the stratigraphic order of partially consolidated beds by the upward or horizontal expulsion of fluid from unconsolidated beds during liquidisation to result in dismembered stratigraphic order. The final bed orientations no longer resemble the original horizontal bedding. Outcrops that show this form of bed structure dominant in Horizon 2 at the Vredefort sites.

They display a variety of the SSDs such as sedimentary dykes, pseudonodules and fragmented bedding reflecting dismemberment during liquidisation and dewatering, with crosscutting fluid escape structures. They are associated with cross-cutting sedimentary dykes and injections sills. A common SSDs in Horizon 2 at the Vredefort study sites is detached and dismembered beds floating in a pelitic matrix.

Sedimentary dykes and plastic intrusions

Small-scale sedimentary dykes and plastic intrusions occur as forceful injections of water-saturated unconsolidated fine-medium grained sand into and/or through partially consolidated pelitic units above. They act as intrusions and often resemble intrusive morphologies, while showing internal flow gradation. They associate with up-drag of the beds adjacent to the sedimentary dyke, and internal turbulence of the injected sand. They occur as escape features when gravity-induced compaction causes the development of vertical bed-scale compaction fractures and/or sedimentary boudinage in pelites.

In the study sites, small-scale sedimentary dykes occur throughout the Parktown Formation but are dominant in Horizon 2. They range in scale from 2 x 0.3 m to small-scale dykes (±10 cm or less). They may crosscut previous dykes or plastic injections suggesting several events of liquidisation. The dykes (and intrusions) are typically ptygmatically folded, which is indicative of progressive compaction, and concomitant dewatering and collapse of the sedimentary pile.

Other plastic injections include small-scale diapirs and sand bulges, or isolated and detached nodules of sand within pelite; these tend to exhibit broadened bases due to progressive compaction. In general, plastic injections extend upwards from underlying beds, but lateral injections are also common. They may be overturned, hooked or ptgmatically folded by progressive compaction (Figure 6e).

Pseudonodules

In the study areas, psuedonodules are present in horizons 1 and 2 (Figures 5b, 6d to f); they display internal bed laminations and/or remnant bedding. The pseudonodules form several morphologies in the study area such as camel-hoof (rhomboidal), square, and rounded to oval shapes. The structures are generally attached to a bedding layer above but may be detached to form isolated floating sand balls.

Slump folds

Soft-sedimentary slump folds form during shear drag (simple shear) on the bedding plane because grain-on-grain contact is lost. The type of folds formed are dependent on the sediment type, and fold forms are invariably modified during the glide/slump event down-slope (e.g., Alsop and Marco, 2013; Alsop et al., 2018). The fold forms can be dismembered during the slumping process. Fold forms may be vergent down-slope; they may associate with micro to mesoscopic fold thrusts and glide planes. They typically associate with dewatering structures and turbulence to produce chaotic bedding.

In the study sites slump folds occur in horizons 2 and 3 of the Parktown Formation. They occur as simple contortions of the bedding rather than complex distortions or dismemberment typical of freeboard slide of bulk material. The slumps are metre-scale in Horizon 3 at the Johannesburg sites (Figures 8a to c), but generally centimetre-scale in horizons 2 and 3 in the Vredefort sites. Slump folds in Horizon 2 at Vredefort are more likely to be bed-scale and dismembered. Preservation of slump folds of centimetre-scale arenite interbeds in pelites is common in Horizon 2. Fold forms range from open to recumbent-isoclinal folds (interlimb angle range from 10° to 85°), or box forms.

Discussion

As stated by Allen (1982), Moretti et al. (2001), Meckel et al. (2007) and Dugan et al. (2012), SSDs document the physical processes that take place during deposition of water-saturated unconsolidated sediments where over-pressuring leads to buoyancy-driven liquidisation (via liquefaction and fluidisation), particularly in heterolithic sediments that resist fluid escape. Liquidisation takes place most commonly in coarse silt to fine sands (Crespellani et al, 1988; Moretti et al., 1999; Owen and Moretti, 2011). This is due to differential cohesion and weight factors limiting grain separation and pore fluid pressures. Liquidisation tends to occur in water-saturated sediments that are loosely packed and display possible permeability barriers such as over-capping with argillaceous sediment (Obermeier, 1996; Owen and Moretti, 2011). Experimental studies by Świątek et al. (2023) suggest that water saturation of greater than 20% volume is needed for SSDs to form.

The process of deposition leads to increased pore fluid pressure during compaction, with concomitant decrease in material strength. The material may change state from solid-to-liquid depending on the rate of dewatering (or degassing) and the degree of loss of grain-on-grain contact. The situation is complicated for unconsolidated interbedded sequences even at the millimetre scale. The processes are rate dependent (Meckel et al., 2007). For example, variations in the rate of top-loading of a sedimentary pile can lead to instability and failure of unconsolidated sediment even at depth if the rate of dewatering is slow relative to the rate of top-loading and rate of pore fluid pressure increase. SSDs are thereby the expressions of rate-dependent loading, dewatering, fluid migration and reworking of the stratigraphic pile.

The SSDs in the study areas dominate three stratigraphic horizons within the Parktown Formation. The assemblage of SSD textures in these horizons correlate well with textures formed during liquidisation by static liquefaction as described and discussed by Allen (1982), relative to formation by dynamic or cyclic liquefaction. We did not find consistent evidence to support inflow of fluid into the system or bulk volume change for liquidisation by fluidisation apart from several large sand dykes (Figure 7a). This may suggest limited fluidisation. Rather, the dominant SSD textures in horizons 1 to 3 relate to simple dewatering of the sedimentary pile and concomitant reworking (in staged events). Soft-sedimentary dewatering channels, load casts, attached and detached pseudonodules, small-scale dykes and plastic intrusions (sand diapers and bulges), syn-sedimentary microfaults, and floating lithons were the inevitable products of static liquefaction.

As a rule, the trigger mechanisms to liquidisation (leading to either liquefaction or fluidisation) are difficult to constrain particularly in ancient rocks. Unfortunately, there is a tendency in the literature to link SSD textures directly to earthquake activity or other forms of tectonically induced seismicity (Shanmugam, 2016, 2017 and references therein). However, Shanmugam (2017) warns against trigger identification, i.e., SSDs are the products of liquidisation, and liquidisation is not unique to single geological-hydrodynamic process(es). In fact, liquidisation may occur through internal build-up of water pressure, sediment loading, geochemical changes in bed profiles (quick clays of Rankka et al., 2004), wave action, slope angle and slope angle changes, earthquakes and other tectonic processes that generate tremors, or combinations of the above. In reality, it is not possible to refine the causes to liquidisation without contextualising the geology.

In that regards, Frimmel (2019) and Nwaila et al. (2017) have made the case for deposition of the Lower West Rand Group in a passive margin setting, and Smith et al. (2013), Viehmann et al. (2015) and Nwaila et al. (2017) have demonstrated that the iron formations such as the Water Shale and Contorted Bed are deposited in quiet-water, offshore, shallow marine environments. These environments tend to be aseismic discounting the possibility that intraplate earthquakes can occur in passive margin settings, but are infrequent (Stein et al., 1989; Balcerak, 2012). However, we did not find evidence in the study areas to correlate the SSDs to cyclic liquefaction, or indeed any form of bed-load reversal associated with earthquake or wave action.

Moreover, although turbidite beds occur throughout the Parktown Formation they are finely-bedded distal facies turbidites; they indicate instabilities in distal regions of the depocenter (basin), or small-scale failures. The slump-folded beds found in horizons 2 and 3 are simple contortions of the bedding. They do not give evidence of down-slope or freeboard slide of bulk material, as occurs in turbidite currents (Shanmugam, 2019). In any event, the presence of slump folds and turbidites cannot be conclusively linked to seismicity or wave action in ancient passive margins. It is also difficult to establish whether slope changes acted as a trigger mechanism because topographic or offshore bathymetric changes cannot be tested for ancient passive margins.

Rather, the SSDs and their lithostratigraphy in the study areas supports fluctuations in overburden pressure and capped dewatering leading to increased pore fluid pressure and ultimately static liquefaction, i.e., the trigger was the static load and purely autogenic in the quiet-water and offshore, shallow marine environment that was the early West Rand Group basin. Exogenic triggers are not indicated.

We thereby link static liquefaction in the Parktown Formation to capped dewatering with cyclic fluctuations in the pore fluid pressure, i.e., dewatered fluid could not easily escape but was capped by Fe-rich argillaceous beds leading to increased pore fluid pressure and repeated cycles of failure. In our model, slow or restricted dewatering below Fe-rich argillaceous horizons (as over-capping) caused an effective increase in pore fluid pressure in ponded water resulting in static liquefaction and development of the SSD features.

Of concern for this interpretation is the spatial distribution of horizons 1-3 across the broader West Rand Group of the Witwatersrand Basin (Figure 1). The Water Tower Shale (Horizon 1) and Contorted Bed (Horizon 3) are marker units in the generalised stratigraphy of the Witwatersrand Basin (SACS, 2006), which is estimated to be 350 long x 200 km wide. For example, the Contorted Bed has been mapped across most of the basin (Hatch and Corstorphine, 1905; Mellor 1911; Fripp and Gay, 1972; Camden-Smith, 1980; Mayer and Albat, 1990; Smith et al., 2013). It follows that triggers to regional static liquefaction in key horizons must have been regionally consistent, persistent and repeated. We propose that static liquefaction was an integral part of sediment deposition on the Parktown Formation offshore platform along the edge of the passive margin (*c.f.* Nwaila et al., 2017; Frimmel, 2019), but has not previously been recognised as important in the reworking of the West Rand Group stratigraphy in the Witwatersrand basin.

Conclusions

Models by Watchorn (1980), Camden-Smith (1980), McCarthy (2006), Nwaila et al. (2017) and Frimmel (2019) for deposition of the Parktown Formation in a passive margin setting have focussed on the overall heterolithic stratigraphy, flow-direction indicators in arenaceous units, and litho-geochemistry of argillite and BIF beds to promote the progradation of distal shelf deposits during early deposition in the lower West Rand Group. Our approach has been to add SSDs found in the Parktown Formation to further develop an understanding of early basin development in the passive margin into which the sediments where deposited.

We recognise the presence of SSDs throughout the Parktown Formation but report their dominance in three stratigraphic horizons in the West Rand Group; Horizon 3 is the regional marker known as the Contorted Bed. They include small- and large-scale dewatering channels, sedimentary dykes, intricately slumped and chaotic beds, pseudonodules, floating lithons, and load casts. The character and makeup of the SSDs corresponds well to dewatering and staged reworking of the sedimentary pile during static liquefaction on the Parktown Formation offshore platform; the trigger mechanism to liquefaction was the static load and capping by argillaceous sediments, and purely autogenic.

Importantly, syn-sedimentary slump folds in horizons 2 and 3 (the Contorted Bed) of the Parktown Formation are limited to bed-scale slip, or simple collapse and rotation of beds over metre intervals, rather than bulk collapse and freeboard displacement. The slump folds in the Contorted Bed are crosscut by faults, and tectonically induced vergent fold-thrusts and axial planar cleavages. These have historically caused some confusion in understanding the Contorted Bed.

Acknowledgements

The authors acknowledge the support of C. Meyer of Kopjeskraal Country Lodge for his hospitality and assistance in gaining access to Donkervliet Eko and Avontuursentrum, the staff at Donkervliet Eko and Avontuursentrum for their kindness and welcoming nature, G. Benade of The Dome Arts Retreat for granting unlimited access to Deelfontein, and Mooihoek farms, and A. Tshibubudze for constructive discussions. We acknowledge C. Bentley for giving written permission to use his photographs of the Contorted Bed along the Jan Smuts Road section. The authors thank Bertus Smith and an anonymous reviewer for detailed and considered reviews of the manuscript, which greatly improved the quality of the work.

References

Allen, J.R.L., 1982. Sedimentary Structures: Their Character and Physical Basis. Unabridged one-volume edition. Developments in Sedimentology 30. Elsevier, Amsterdam. Volume I and II, 593p and 663p, respectively.

Alsop, G.I. and Marco, S., 2013. Seismogenic slump folds formed by gravity-driven tectonics down a negligible subaqueous slope. Tectonophysics, 605, 48-69.

Alsop, G.I., Weinberger, R.S., Marco, S. and Levi, T., 2018. Folding during soft-sediment deformation. Geological Society, London, Special Publications, 487, 81-104.

Armstrong, R.A., Compston, W., Retief, E.A., Williams, I.S. and Welke, H.J., 1991. Zircon ion microprobe studies bearing on the age and evolution of the Witwatersrand triad. Precambrian Research, 53, 243-266.

Balcerak, E., 2012. Passive margin earthquakes: Reviewing knowledge and challenges. EOS, 93, 132-132.

Beaton, K.J., Gibson, R.L., Bybee, G.M., Walker, S., Diener, J.F.A. and Baxter, E.F., 2022. Amphibolite facies metamorphism in lower Witwatersrand Supergroup rocks exposed in the Vredefort Dome – a Ventersdorp LIP connection. South African Journal of Geology, 125, 191-210.

Boggs, S., 2011. Principles of Sedimentology and Stratigraphy: Fifth Edition. Pearson Prentice Hall, New Jersey, 585pp

Camden-Smith, P.M., 1980. The Sedimentology, Geochemistry and Diagenesis of West Rand Group Sediments in the Heidelberg Area, Transvaal. Unpublished MSc. thesis, University of Cape Town, South Africa, 232pp

Crespellani, T., Nardi, R. and Simoncini, C., 1988. La liquefazione del terreno in condizioni sismiche. Zanichelli, Bologna, 185pp

Dankert, B.T. and Hein K.A.A., 2010. Evaluating the structural character and tectonic history of the Witwatersrand Basin. Precambrian Research, 177, 1-22.

Draper, D., 1896. The Primary Systems of South Africa with special reference to the conglomerate beds of the Witwatersrand. Transactions of the Geological Society of South Africa, 1, 12-26.

Dugan, B. and Sheahan, T.C., 2011. Offshore sediment overpressures of passive margins: mechanisms, measurement, and tools. Reviews of Geophysics, 50, RG3001, pp. 2011RG000379

Ettensohn, F.R., Rast, N. and Brett, C.E., 2002. Ancient Seismites. Geological Society of America, Special Paper, 359.

Frimmel, H.E., 2019. The Witwatersrand Basin and Its Gold Deposits. In: A. Kröner and A. Hofmann (Editors), The Archaean Geology of the Kaapvaal Craton, Southern Africa. Regional Geology Reviews. Springer, Cham. https://doi.org/10.1007/978-3-319-78652-0_10

Fripp, R.E.P. and Gay, N.C., 1972. Some structural aspects of the Hospital Hill Series on the north-central margin of the Witwatersrand Basin. Transactions of the Geological Society of South Africa, 75, 189-196.

Hansen, L., Eilertsen, R.S., Solberg, I.L., Sveian, H. and Rokoengen, K., 2007. Facies characteristics, morphology and depositional models of clay-slide deposits in terraced fjord valleys, Norway. Sedimentary Geology, 202, 710-729.

Hatch, F.H. and Corstorphine, S., 1905. The Geology of the Bezuidenhout Valley and the district east of Johannesburg. Transactions of the Geological Society of South Africa, 7, 97-109.

Jackson, J.A. and Bates, R.L., 1997. Glossary of Geology, 4th Edition, American Geological Institute, Alexandria, 769pp

Jones, M.E. and Preston, R.M.F., 1987. Deformation of Sediments and Sedimentary Rocks. Geological Society Special Publication No. 29, 350pp

Kositcin, N. and Krapez, B., 2004. Relationship between detrital zircon age-spectra and the tectonic evolution of the Late Archaean Witwatersrand Basin, South Africa. Precambrian Research, 129, 141-168.

Lowe, D.R., 1975. Water escape structures in coarse-grained sediments. In: Sedimentology, 22, 157-204.

Macar, P., 1948. Les pseudo-nodules du Famennien et leur origine. Annales de la Société Géologique de Belgique, 72B, 47-74.

Maltman, A., 1994. The Geological Deformation of Sediments. Chapman and Hall, London, 362pp

Maltman, A.J., Hubbard, B. and Hambrey, M.J., 2000. Deformation of Glacial Materials. Geological Society, London, Special Publications, 176pp

Manzi, M.S.D., Hein, K.A.A., King, N. and Durrheim, R.J., 2013. Neoarchaean tectonic history of the Witwatersrand Basin and Ventersdorp Supergroup: New constraints from high-resolution 3D seismic reflection data. Tectonophysics, 590, 94-105.

Mashabela, S., 2016. Analysis of pre-impact and impact-induced geological structures in the northern collar of the Vredefort dome, South Africa. Unpublished MSc thesis, University of the Witwatersrand Johannesburg, 187p

Mayer, J.J. and Albat, H.M., 1990. A appraisal of the significance of small-scale folding structures in the contorted bed of the area of the Vredefort structure. South African Journal of Geology, 93, 311-317.

McCarthy, T.S., 2006. The Witwatersrand Supergroup, In: M.R. Johnson, C.R. Anhaeusser, and R.J. Thomas (Editors), The Geology of South Africa. The Geological Society of South Africa, Johannesburg and Council for Geoscience, Pretoria, 155-186.

Meckel, T.A., Ten Brink, U.S. and Williams, S.J., 2007. Sediment compaction rates and subsidence in deltaic plains: numerical constraints and stratigraphic influences. Basin Research, 19, 19-31.

Mellor, E.T., 1911. Some structural features of the Witwatersrand System on the Central Rand, with a note on the Rietfontein Series. Transactions of the Geological Society of South Africa, Volume XIV, 24-42.

Molezzi, M., 2017. Modelling The Witwatersrand Basin: A window into Neoarchaean-Palaeoproterozoic crustal-scale tectonics. Unpublished MSc. thesis, University of the Witwatersrand Johannesburg, 223pp

Molezzi, M.G., Hein, K.A.A. and Manzi, M.S.D., 2019. Mesoarchean-Palaeoproterozoic crustal scale tectonics of the central Witwatersrand basin – Interpretation from 2D seismic data and 3D geological modelling. Tectonophysics, 761, 65-68.

Moretti, M. and Van Loon, A.J., 2014. Restrictions to the application of 'diagnostic' criteria for recognizing ancient seismites. Journal of Paleogeography, 3, 162-173.

Moretti, M., Alfaro, P., Caselles, O. and Canas, J.A., 1999. Modelling seismites with a digital shaking Table. Tectonophysics, 304, 369-383.

Moretti, M., Soria, J.M., Pedro, A. and Walsh, N., 2013. Asymmetrical soft-sediment deformation structures triggered by rapid sedimentation in turbiditic deposits (Late Miocene, Guadix Basin, southern Spain) Facies, 44, 283-294.

Nwaila, G., Frimmel, H.E. and Minter, W.E.L., 2017. Provenance and Geochemical Variations in Shales of the Mesoarchean Witwatersrand Supergroup. The Journal of Geology, 125, 399-422.

Obermeier, S.F., 1996. Use of liquefaction-induced features for paleoseismic analysis. Engineering Geology, 44, 1-76.

Owen, G., 1978. Pseudonodules. In: Sedimentology. Encyclopedia of Earth Science. Springer, Berlin, Heidelberg, 549-551.

Owen, G. and Moretti, M., 2011. Identifying triggers for liquefaction-induced soft sediment deformation in sands. Sedimentary Geology, 235, 141-147.

Owen, G., Moretti, M. and Alfaro, P., 2011. Recognizing triggers for soft-sediment deformation: Current understanding and future directions. Sedimentary Geology, 235, 133-140.

Owen, G., 1987. Deformation processes in unconsolidated sands. In: M.E. Jones, and R.M.F. Preston (Editors), Deformation of Sediments and Sedimentary Rocks, Geological Society, London, Special Publication, 29, 11-24.

Penning, W.H., 1891. A contribution to the geology of the Southern Transvaal. Quarterly Journal of the Geological Society of London, 70, 451-46l.

Potter, P.E. and Pettijohn, F.J., 1963. Paleocurrents and Basin Analysis. Springer-Verlag, New York, 460pp

Pretorius, D.A., Brink, W.C.J. and Fouche, J., 1986. Geological map of the Witwatersrand Basin. In: C.R. Anhaeusser and S. Maske (Editors), Mineral Deposits of Southern Africa, Vol. I. Geological Society of South Africa, Johannesburg.

Rankka, K., Andersson-Sköld, Y., Hultén, C., Larsson, R., Leroux, V. and Dahlin, T., 2004. Quick clay in Sweden. Report 65, Swedish Geological Institute, 145pp

Reimold, W.U. and Gibson, R.L., 2006. The melt rocks of the Vredefort impact structure – Vredefort Granophyre and pseudotachylitic breccias: implications for impact cratering and the evolution of the Witwatersrand Basin. Chemie der Erde - Geochemistry 66, 1-35.

SACS, 2006. A revised stratigraphic framework for the Witwatersrand Supergroup, South African Committee for Stratigraphy (SACS) Task Group for the Witwatersrand Supergroup. Lithostratigraphic Series No 42, 26pp

Shanmugam, G., 2016. The seismite problem. Journal of Palaeogeography, 5, 318-362.

Shanmugam, G., 2017. Global case studies of soft-sediment deformation structures (SSDs): definitions, classification, advances, origins, and problems. Journal of Palaeogeography, 6, 251-320.

Shanmugam, G., 2019. Slides, Slumps, Debris Flows, Turbidity Currents, Hyperpycnal Flows, and Bottom Currents. In: J.K. Cochran, H.J. Bokuniewicz and P.L. Yager (Editors), Encyclopedia of Ocean Sciences, Volume 4, 228-257.

Smith, A.J.B., Gutzmer, J., Beukes, N.J., Reinkie, C. and Bau, M., 2008. Rare earth elements (REE) in banded iron formations–link between geochemistry and mineralogy. Australian Institute for Mining and Metallurgy (AusIMM), 9th International Congress for Applied Mineralogy, Brisbane, Australia, 8-10 September 2008, Proceedings, 651-658.

Smith, A.J.B., Beukes, N.J. and Gutzmer, J., 2013. The composition and depositional environments of Mesoarchean iron formations of the West Rand Group of the Witwatersrand Supergroup, South Africa. Economic Geology, 108.1, 111-134.

Stanistreet, I.G. and McCarthy, T.S., 1991. Changing tectono-sedimentary scenarios relevant to the development of the Late Archaean Witwatersrand Basin. Journal of African Earth Sciences, 13, 65-81.

Stein, S., Cloetingh, S., Sleep, N.H. and Wortel, R., 1989. Passive margin earthquakes, stresses and rheology. In: S. Gregersen and P.W. Basham, (Editors), Earthquakes at North Atlantic passive margins: Neotectonics and postglacial rebound, Springer, 1989.

Stevens, G., Boer, R. and Gibson, R., 1997. Metamorphism, fluid-flow, and gold mobilization in the Witwatersrand Basin: towards a unifying model. South African Journal of Geology, 100, 363-375.

Struben, F.P.T., 1885. A geological section of the Witwatersrand. Reported anonymously in Transactions of the Geological Society of South Africa, 50, 177-178.

Świątek, S., Belzyt, S., Pisarska-Jamroży, M. and Woronko, B., 2023. Sedimentary records of liquefaction: Implications from field studies. Journal of Geophysical Research: Earth Surface, 128, e2023JF007152. https://doi.org/10.1029/2023JF007152

Truswell, J.F., 1970. An introduction to the historical geology of South Africa. Purnell, Cape Town, 167pp

Viehmann, S., Bau, M., Smith, A.J.B., Beukes, N.J., Elton L. Dantas, E.L. and Bühn, B., 2015. The reliability of ~2.9 Ga old Witwatersrand banded iron formations (South Africa) as archives for Mesoarchean seawater: Evidence from REE and Nd isotope systematics. Journal of African Earth Sciences, 111, 322-334.

Vos, R.G., 1975. An alluvial plain and lacustrine model for the Precambrian Witwatersrand deposits of South Africa. Journal Sedimentary Research, 45, 480-493.

Wang, C. and Manga, M., 2021. Water and Earthquakes. Lecture notes in Earth System Sciences, Springer ISSN 2193-8571, 46-49.

Watchorn, M.B., 1980. The Stratigraphic and Sedimentological Development of the Witwatersrand West Rand Basin in the Klerksdorp area. Economic Geology Research Unit, 148, 1-9.

Editorial handling: M.A. Elburg.